DOI: 10.1111/j.1467-8659.2010.01735.x

Eurographics Symposium on Rendering 2010
Jason Lawrence and Marc Stamminger
(Guest Editors)

Volume 29 (2010), Number 4

A New Ward BRDF Model with Bounded Albedo

David Geisler-Moroder and Arne Dür†

University of Innsbruck, Austria

Abstract

Due to its realistic appearance, computational convenience, and efficient Monte Carlo sampling, Ward's anisotropic BRDF is widely used in computer graphics for modeling specular reflection. Incorporating the criticism that the Ward and the Ward-Dür model do not meet energy balance at grazing angles, we propose a modified BRDF that is energy conserving and preserves Helmholtz reciprocity. The new BRDF is computationally cheap to evaluate, admits efficient importance sampling, and thus sustains the main benefits of the Ward model. We show that the proposed BRDF is better suited for fitting measured reflectance data of a linoleum floor used in a real-world building than the Ward and the Ward-Dür model.

Categories and Subject Descriptors (according to ACM CCS): I.3.7 [Computer Graphics]: Three-Dimensional Graphics and Realism—Color, shading, shadowing, and texture

1. Introduction

A bidirectional reflectance distribution function (BRDF) [NRH*77] $f(\theta_l, \varphi_l; \theta_v, \varphi_v)$ describes the reflectance properties of a surface by specifying the amount of radiance incident from direction (θ_l, φ_l) that is reflected into direction (θ_v, φ_v), i.e.,

$$L_v(\theta_v, \varphi_v) = \int_0^{2\pi} \int_0^{\pi/2} L_l(\theta_l, \varphi_l) f(\theta_l, \varphi_l; \theta_v, \varphi_v) \cos\theta_l \sin\theta_l \, d\theta_l \, d\varphi_l. \quad (1)$$

The main characteristics of a *physically plausible* BRDF are *Helmholtz reciprocity* and *energy conservation* [Lew94]. Helmholtz reciprocity stands for the symmetry between incident and reflected directions,

$$f(\theta_l, \varphi_l; \theta_v, \varphi_v) = f(\theta_v, \varphi_v; \theta_l, \varphi_l), \quad (2)$$

that allows global illumination calculations by backward ray tracing algorithms [Whi80]. Energy conservation – or *energy balance* – means that the *albedo*, i.e., the total reflected power for a given direction of incident radiation,

$$a(\theta_l, \varphi_l) = \int_0^{2\pi} \int_0^{\pi/2} f(\theta_l, \varphi_l; \theta_v, \varphi_v) \cos\theta_v \sin\theta_v \, d\theta_v \, d\varphi_v \quad (3)$$

is bounded by 1.

Over the last five decades numerous BRDF models were introduced. Beckmann [BS63] and Torrance and Sparrow [TS67] presented physically based microfacet BRDF models that use the Gaussian distribution to define the microfacets' surface normals. The model by Torrance and Sparrow was used in computer graphics by Cook and Torrance [CT81] and later improved by He et al. [HTSG91]. However, these models are neither suitable for Monte Carlo integration due to missing efficient importance sampling formulae, nor do they provide anisotropic reflection. The first empirical and probably most famous model that simulates specular reflections was introduced by Phong [Pho75] and later improved by Blinn [Bli77]. Other physically plausible BRDFs that model anisotropic reflection and are suitable for Monte Carlo integration were proposed by Schlick [Sch94], Lafortune et al. [LFTG97], Ashikmin and Shirley [AS00], and Kurt et al. [KSKK10].

As a simplification of the Cook-Torrance model, Ward [War92] presented an anisotropic BRDF that was later improved by Dür [Dür06]. The main benefits of this model are that it is computationally cheap to evaluate, it admits efficient importance sampling for Monte Carlo integration, and it is simple and intuitive to use with only three parameters, one for specularity and two for roughness. Neumann et al. [NNSK99] proposed modifications for the Phong, Blinn,

† email: {David.Geisler-Moroder | Arne.Duer}@uibk.ac.at

and Ward models by specifying correction terms to make them physically plausible.

2. The Ward-Dür BRDF and its Sampling

In [War92], Ward proposes a BRDF that models anisotropic specular reflection by

$$f_{\mathrm{W}}(\theta_l, \varphi_l; \theta_v, \varphi_v) = \frac{\rho_s}{} \cdot \exp\left(-\tan^2\Delta\left(\frac{\cos^2\varphi}{\alpha_x^2} + \frac{\sin^2\varphi}{\alpha_y^2}\right)\right) \cdot \frac{1}{4\sqrt{\cos\theta_l \cos\theta_v}}, \tag{4}$$

where (θ_l, φ_l), (θ_v, φ_v), and (Δ, φ) denote the polar and azimuthal angles of the incident and reflected directions, and of the halfway vector, respectively (see Figure 1). The material properties are given by the *specular reflectance* ρ_s and by the *roughness* values α_x and α_y that equal $\sqrt{2}$ times the standard deviations in the perpendicular directions $\vec{x}$ and $\vec{y}$ of the 2D Gaussian distribution.

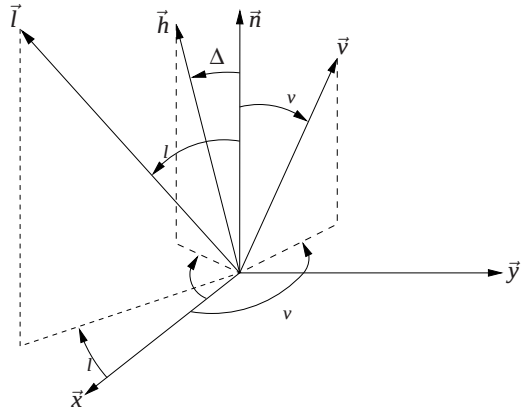

Figure 1: *Polar and azimuthal angles: $\vec{n}$ is the surface normal, $\vec{l}$ is the light source or sampling direction, $\vec{v}$ is the view point direction, and $\vec{h}$ is the halfway vector. All vectors have unit length, and azimuthal angles are negative iff oriented from $\vec{y}$ to $\vec{x}$.*

Based on investigations on the energy balance of Ward's reflection model, Dür [Dür06] presents an improved normalization for the Ward BRDF that we refer to as Ward-Dür BRDF:

$$f_{\mathrm{WD}}(\theta_l, \varphi_l; \theta_v, \varphi_v) = \frac{\rho_s}{} \cdot \exp\left(-\tan^2\Delta\left(\frac{\cos^2\varphi}{\alpha_x^2} + \frac{\sin^2\varphi}{\alpha_y^2}\right)\right) \cdot \frac{1}{4\cos\theta_l \cos\theta_v}. \tag{5}$$

Following *Ward's sampling method* [War92, WS98], for a given reflected direction $\vec{v} = (\theta_v, \varphi_v)$ the incident direction $\vec{l} = (\theta_l, \varphi_l)$ is determined via the halfway vector $\vec{h}$ that is given by its angles

$$\Delta = \arctan\left(\sqrt{\frac{-\log(1-s)}{\cos^2\varphi/\alpha_x^2 + \sin^2\varphi/\alpha_y^2}}\right) \quad \text{and}$$
$$\varphi = \operatorname{atan2}(\alpha_y \sin(2\pi t), \alpha_x \cos(2\pi t)), \tag{6}$$

where s and t are independent random numbers uniformly distributed in $[0,1)$ (compare [Dür06, Wal05]). Dür shows that the distribution of the random direction $\vec{l}$ has the probability density function (PDF)

$$\mathrm{d}_{\omega}(\theta_l, \varphi_l; \theta_v, \varphi_v) = \frac{f_{\mathrm{WD}}(\theta_l, \varphi_l; \theta_v, \varphi_v)}{s \cdot w(\theta_l, \varphi_l; \theta_v, \varphi_v)}, \tag{7}$$

with

$$w(\theta_l, \varphi_l; \theta_v, \varphi_v) = \frac{(\cos\theta_l + \cos\theta_v)^3}{4\cos\theta_v (1 + \cos\theta_l \cos\theta_v + \sin\theta_l \sin\theta_v \cos(\varphi_v - \varphi_l))}. \tag{8}$$

Because at non-grazing angles and for small values of α_x and α_y

$$\mathrm{d}_{\omega}(\theta_l, \varphi_l; \theta_v, \varphi_v) \approx f_{\mathrm{WD}}(\theta_l, \varphi_l; \theta_v, \varphi_v) / \rho_s, \tag{9}$$

weighting factors are mostly neglected in the Monte Carlo integration (for details on the implementation in RADIANCE [War94, WS98] see [GMD10]). However, at grazing angles the difference between the BRDF f_{WD} and the sampling PDF d_{ω} is significant and can be clearly observed in Figure 2. Figure 2(a) shows the set-up of a test scene where a gray isotropic surface with 80% specular reflection (ρ_d = 0.12, ρ_s = 0.48) and roughness $\alpha_x = \alpha_y = 0.1$ is viewed at a grazing angle of 1°. Below, the luminance distributions that result if the direct illumination is computed by evaluating the Ward-Dür BRDF (Figure 2(b)) or by using Ward's sampling method (Figure 2(c)) are juxtaposed.

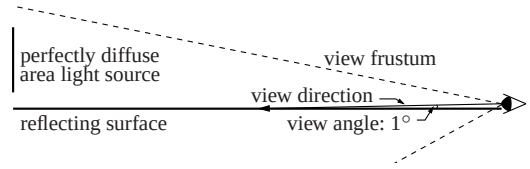

(a)

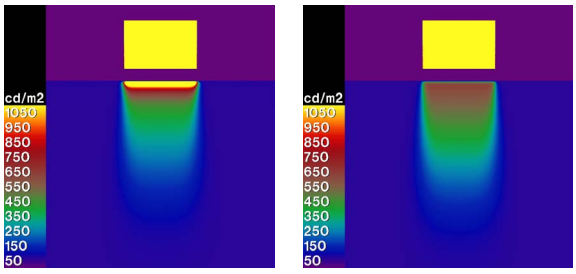

(b) (c)

Figure 2: *Grazing angle test scene: (a) set-up, and luminance distributions resulting from (a) Ward-Dür BRDF and (b) Ward's sampling method.*

In [NNSK99] Neumann et al. criticize that the Ward BRDF is not physically plausible because at grazing angles the BRDF diverges to infinity and its albedo violates energy

balance, i.e. is greater than 1. Using $\max(\cos\ _l, \cos\ _v)$ instead of $\sqrt{\cos\ _l \cos\ _v}$ in Equation (4), Neumann et al. propose a modification that meets energy balance but still has the shortcoming that specular highlights are too dark, especially for low-lying light sources. We refer to this modification as Ward-Neumann BRDF.

Because the Ward-Dür BRDF can be written as $f_{\mathrm{WD}}(\vec{l},\vec{v}) = f_{\mathrm{W}}(\vec{l},\vec{v})/\sqrt{\cos\ _l \cos\ _v}$ the lower bound argument that proves the divergence of the albedo of the Ward BRDF at grazing angles in Equation (41) in [NNSK98] also holds for the Ward-Dür BRDF. In Figure 6 the albedos of the Ward-Neumann BRDF, the Ward BRDF, the Ward-Dür BRDF, our new BRDF, and the PDF of Ward's sampling method are compared.

3. A New BRDF

Motivated by the discrepancy between the evaluation of the Ward-Dür BRDF and the sampling by Ward's method, and to account for the criticism by Neumann et al. [NNSK99], we propose the following modification of the Ward-Dür BRDF that preserves Helmholtz reciprocity:

$$f_{new}(\ _l,\ _l;\ _v,\ _v) = \frac{\ _s}{} \cdot \exp\left(-\tan^2\Delta\left(\frac{\cos^2}{2} + \frac{\sin^2}{2}\right)\right) \cdot \frac{2\,(1+\cos\ _l\cos\ _v + \sin\ _l\sin\ _v\cos(\ _v - \ _l))}{(\cos\ _l + \cos\ _v)^4}. \quad (10)$$

Expressing the BRDF as

$$f_{new}(\ _l,\ _l;\ _v,\ _v) = \frac{\ _s}{} \cdot \quad (11)$$

$$\exp\left(-\frac{1}{\langle\vec{l}+\vec{v},\vec{n}\rangle^2}\cdot\left(\frac{\langle\vec{l}+\vec{v},\vec{x}\rangle^2}{\ _2} + \frac{\langle\vec{l}+\vec{v},\vec{y}\rangle^2}{\ _2}\right)\right)\cdot\frac{1}{4\langle\vec{l},\vec{h}\rangle^2\langle\vec{h},\vec{n}\rangle^4}$$

proves that the new BRDF is different from both the Beckmann distribution [BS63] and the model by Kurt, Szirmay-Kalos, and Křivánek [KSKK10]. Compared to the Ward-Dür BRDF, the factor $\langle\vec{l},\vec{n}\rangle\langle\vec{v},\vec{n}\rangle$ in the denominator of Equation (5) is replaced by $\langle\vec{l},\vec{h}\rangle\langle\vec{v},\vec{h}\rangle\langle\vec{h},\vec{n}\rangle^4 = \langle\vec{l},\vec{h}\rangle^2\langle\vec{h},\vec{n}\rangle^4$.

The polar plots in Figures 3 and 4 compare the isotropic BRDF of our proposed model to the Ward and the Ward-Dür model for roughness values $\quad = \quad = 0.1$ or $\quad = \quad = 0.2$ in the plane of incidence. From Figures 3 and 4 one can see that the new BRDF mainly coincides with the Ward-Dür BRDF but does not diverge to infinity at grazing angles. The polar plots in Figure 5 compare the BRDFs for constant polar angles. The coincidence of the Ward-Dür BRDF and the new BRDF in Figure 5 also indicates that for realistic roughness values and up to 0.25 the two BRDFs almost match. In particular

$$f_{new}(\ _l,\ _l;\ _l,\ _l + \ ) = \frac{\ _s}{4\quad\cos^2\ _l} = f_{\mathrm{WD}}(\ _l,\ _l;\ _l,\ _l + \ ). \quad (12)$$

Figures 3 and 4 predict that, in the plane of incidence, the maximum of the BRDF $f_{new}(\vec{l},\vec{v})$ occurs below the mirror direction, whereas the maximum of the BRDF times the cosine of the polar angle of the reflected direction $f_{new}(\vec{l},\vec{v})\cdot\cos\ _v$ is located in the mirror direction (the corresponding proofs are given in the appendix). Thus, the new BRDF shows the same behaviour as the Ward-Dür BRDF concern-

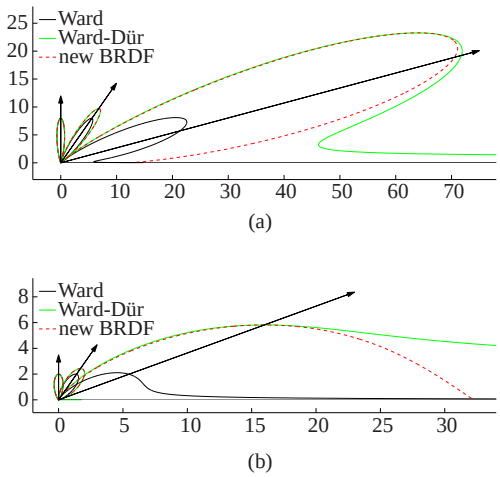

Figure 3: *Ward BRDF, Ward-Dür BRDF, and new BRDF at* $\ _l = 0°, 35°$, *and* $70°$ *for* $\ _s = 1$ *and (a)* $\quad = \quad = 0.1$ *and (b)* $\quad = \quad = 0.2$.

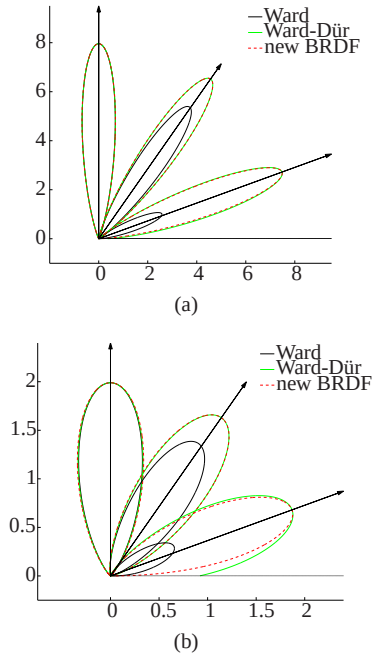

Figure 4: *BRDF multiplied by* $\cos\ _l$ *and* $\cos\ _v$ *for Ward BRDF, Ward-Dür BRDF, and new BRDF at* $\ _l = 0°, 35°$, *and* $70°$ *for* $\ _s = 1$ *and (a)* $\quad = \quad = 0.1$ *and (b)* $\quad = \quad = 0.2$.

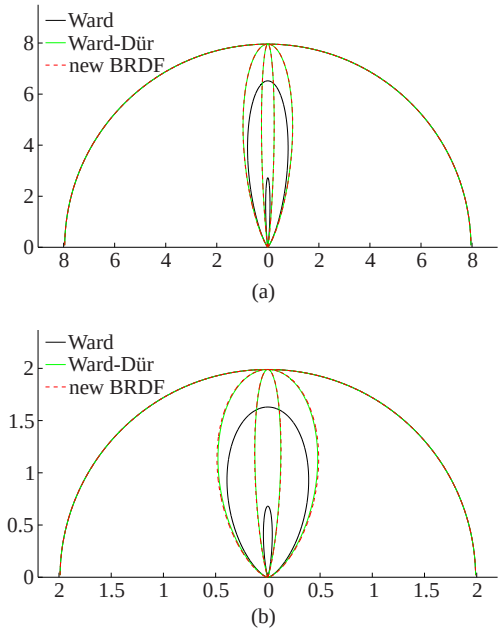

Figure 5: *Azimuthal variation at* $\theta_l = \theta_v = 0°, 35°,$ *and* $70°$ *(outside to center) of BRDF multiplied by* $\cos\theta_l$ *and* $\cos\theta_v$ *for Ward BRDF, Ward-Dür BRDF, and new BRDF for* $\rho_s = 1$ *and (a)* $\alpha_x = \alpha_y = 0.1$ *and (b)* $\alpha_x = \alpha_y = 0.2$.

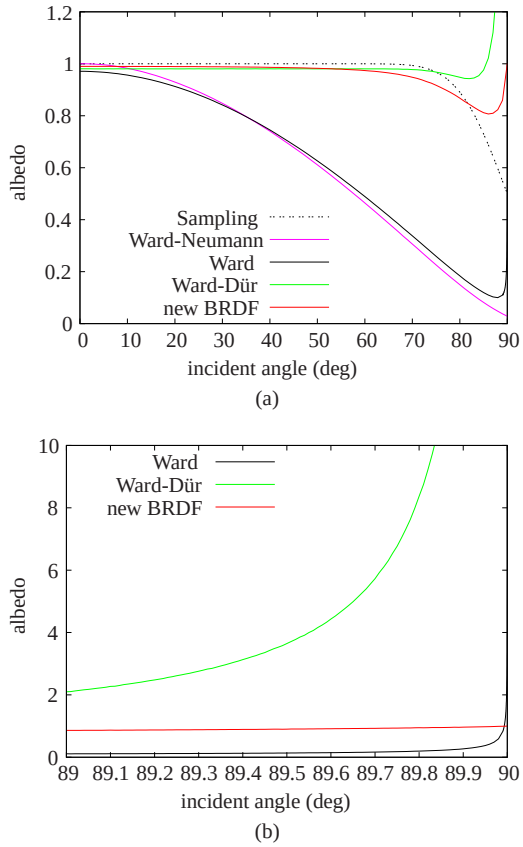

Figure 6: *Albedo functions for* $\rho_s = 1$ *and* $\alpha_x = \alpha_y = 0.1$ *: (a) for various BRDF models and (b) at grazing angles for the Ward BRDF, the Ward-Dür BRDF, and the new BRDF.*

ing off-specular peaks that were first described by Torrance and Sparrow [TS67].

Figures 6 and 7 provide numerical evidence that our proposed BRDF model meets energy balance, i.e. the albedo is bounded by 1: for all $\theta_l \in [0, \pi/2)$

$$a(\theta_l, \alpha_l) = \int_0^2 \int_0^{\pi/2} f_{new}(\vec{l}, \vec{v}) \cos\theta_v \sin\theta_v \, d\theta_v \, d\varphi_v \leq 1. \qquad (13)$$

In the appendix we show that the albedo is close to 1 for small roughness values and non-flat angles, and we prove that the albedo converges to 1 for $\theta_l \to \pi/2$.

In Figure 6(a) the albedo functions of the Ward-Neumann BRDF, the Ward BRDF, the Ward-Dür BRDF, the new BRDF, and the PDF of Ward's sampling method are compared in the isotropic case for roughness values $\alpha_x = \alpha_y = 0.1$ and specular reflectance $\rho_s = 1$. Note that the albedo of the sampling method is calculated as $a(\vec{v})$ because in backward ray tracing $\vec{v}$ is the incident direction and $\vec{l}$ is the sampled direction. Because the probability that a direction generated by Ward's sampling method has polar angle $\theta_l < \pi/2$ converges to 1/2 for $\theta_v \to \pi/2$, the albedo of the PDF converges to 0.5 for $\theta_v \to \pi/2$. Figure 6(b) shows the behaviour of the albedo functions for the Ward BRDF, the Ward-Dür BRDF, and the new BRDF at grazing angles. In Figure 7 the albedo functions of our proposed BRDF in the isotropic cases $\alpha_x = \alpha_y = 0.01$, $\alpha_x = \alpha_y = 0.05$, $\alpha_x = \alpha_y = 0.1$, and $\alpha_x = \alpha_y = 0.2$ are presented.

Writing the PDF $d\omega_l$ of Ward's sampling method (see Equation (7)) with respect to our new BRDF yields

$$d\omega_l(\theta_l, \varphi_l; \theta_v, \varphi_v) = \frac{f_{new}(\theta_l, \varphi_l; \theta_v, \varphi_v)}{\rho_s \cdot w_{new}(\theta_l, \varphi_l; \theta_v, \varphi_v)}, \qquad (14)$$

where the weighting factors

$$w_{new}(\theta_l, \varphi_l; \theta_v, \varphi_v) = \frac{2}{1 + \cos\theta_v / \cos\theta_l} = \frac{2}{1 + \langle \vec{v}, \vec{n} \rangle / \langle \vec{l}, \vec{n} \rangle} \qquad (15)$$

are greater (less) than 1 if and only if the sampled direction is above (below) the mirror direction. Then the indirect specular component can be approximated by

$$\int_R L_l(\vec{l}) \, f_{new}(\vec{l}, \vec{v}) \, d\Omega_l \approx \frac{\rho_s}{N} \sum_{n=1}^{N} L_l(\vec{l}^*_{(n)}) w_{new}(\vec{l}^*_{(n)}, \vec{v}), \qquad (16)$$

where R is the area of the hemisphere that is not subtended by light sources, $d\Omega_l = \cos\theta_l \sin\theta_l d\theta_l d\varphi_l$ is the projected surface element, and the directions $\vec{l}^*_{(n)}$ are chosen randomly by Ward's sampling method in Equation (6). Compared to the weighting factors for the Ward-Dür BRDF in Equation (8), the weighting factors w_{new} in Equation (15) are less expensive to compute.

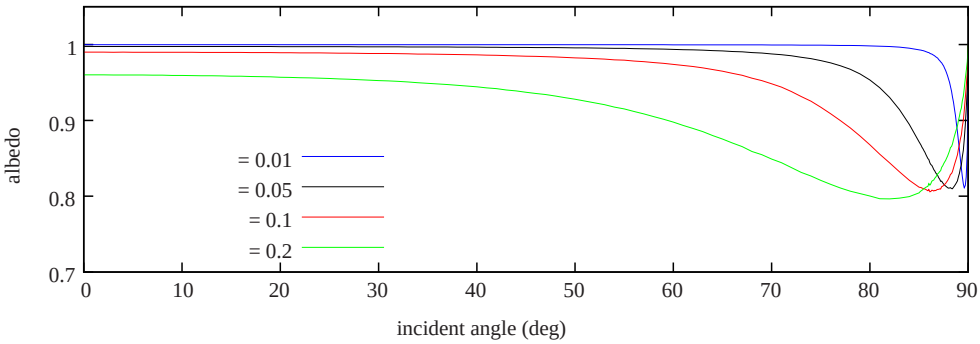

Figure 7: *Albedo functions of the new BRDF for* $_s = 1$ *and varying values of* $\quad = .$

Finally, rewriting Equation (11) as

$$f_{new}(\ _l,\ _l;\ _v,\ _v) = \frac{s}{} \cdot \tag{17}$$

$$\exp\left(-\frac{1}{\langle\vec{l}+\vec{v},\vec{n}\rangle^2}\cdot\left(\frac{\langle\vec{l}+\vec{v},\vec{x}\rangle^2}{2}+\frac{\langle\vec{l}+\vec{v},\vec{y}\rangle^2}{2}\right)\right)\cdot\frac{\langle\vec{l}+\vec{v},\vec{l}+\vec{v}\rangle}{\langle\vec{l}+\vec{v},\vec{n}\rangle^4}$$

shows that the evaluation of the BRDF for the direct specular component

$$\int_S L_l(\vec{l})\, f_{new}(\vec{l},\vec{v})\,\mathrm{d}\Omega_l \approx \sum_{m=1}^{M} L_l(\vec{l}_{(m)})\, f_{new}(\vec{l}_{(m)},\vec{v})\,\Delta\Omega_{l_{(m)}} \tag{18}$$

is computationally cheap and thus sustains one of the main benefits of the Ward model. In Equation (18), S is the area of the hemisphere subtended by light sources and $\vec{l}_{(m)}$ are directions to the light sources.

Grazing Angle Test Scene

We re-rendered the test scene of Section 2 (see Figure 2(a) for the set-up) using Equation (18) for calculating the direct specular component from the light source (Figure 8(a)) or using Equation (16) for computing the indirect specular component from the luminaire now included in the indirect calculation (Figure 8(b)). By using luminance contour lines laid over the images it is clearly visualized that the resulting distributions are the same for the new BRDF and the sampling using the new weighting factors. Including our proposed BRDF and weighting factors in the current version of RADIANCE [Rad10] does not change the rendering times observably.

4. Fitting Measured BRDF Data

The BRDF of an isotropic red linoleum floor was measured with a gonioreflectometer for 222 pairs of incident/outgoing directions by our cooperation partner Bartenbach LichtLabor, Austria [Dür04]. The total reflectance of the isotropic linoleum floor illuminated by the CIE standard illuminant A [CIE04] is 17.5% and was measured by Bartenbach LichtLabor using an integrating sphere.

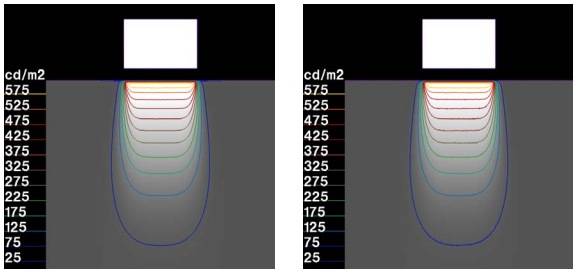

(a) (b)

Figure 8: *Luminance distributions laid over renderings for the Grazing Angle Test Scene: specular reflection calculated (a) by the new BRDF and (b) by Ward's sampling method using new weighting factors.*

For the curve fitting we use a similar approach as Ngan et al. [NDM05], i.e. we define the objective function for fitting as

$$g(\ _l,\ _l;\ _v,\ _v) = \tag{19}$$
$$\left(\text{data}(\ _l,\ _l;\ _v,\ _v) - \left(\frac{d}{} + f(\ _l,\ _l;\ _v,\ _v)\right)\right)\cdot\cos\ _l,$$

where $_d = \ - \ _s$ is the diffuse reflectance, $f = f_W$ for the Ward BRDF, $f = f_{WD}$ for the Ward-Dür BRDF, or $f = f_{new}$ for our proposed BRDF, respectively. The parameter estimation is then performed using the MATLAB routine *lsqnonlin()* that computes $_s$ and $\quad$ such that

$$\sum_{k=1}^{222} g(\ _l^{(k)},\ _l^{(k)};\ _v^{(k)},\ _v^{(k)})^2 \to \min. \tag{20}$$

In Table 1 the results for $_s$ and $\quad$ of the three BRDF models are presented together with the fitting error r that specifies the computed minimum value in Equation (20). Expectedly, compared to the Ward-Dür BRDF we receive a higher value for the roughness $\quad$ that accounts for the tighter lobes of the new BRDF at flat angles (see Figure 3). In turn also the spec-

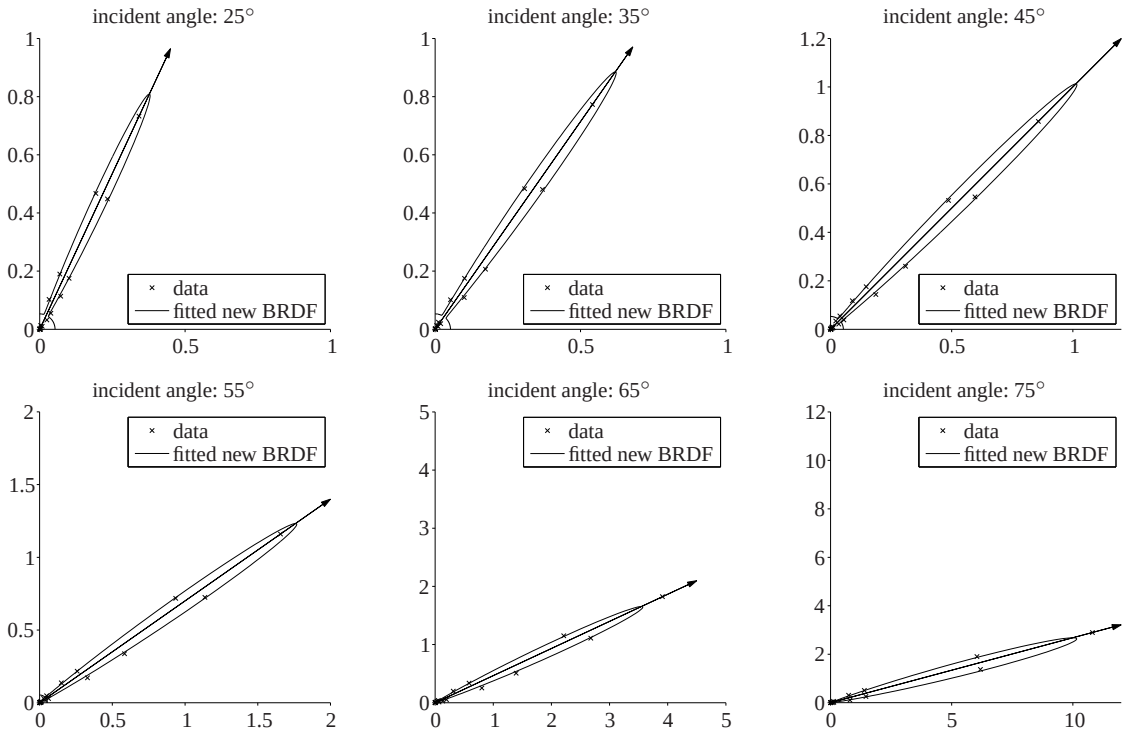

Figure 9: *Measured BRDF data for the isotropic red linoleum floor and fits from the new BRDF model for incident angles from* 25° *to* 75°*. Note the varying scales.*

	Parameter		Error
	s		r
Ward BRDF f_W	0.08508	0.02935	6.8269
Ward-Dür BRDF f_{WD}	0.02605	0.02122	2.8846
proposed BRDF f_{new}	0.04982	0.03172	0.9241

Table 1: *Fitting results for an isotropic red linoleum floor.*

ularity $_s$ increases and thus corrects the length of the lobe that is shortened by the greater . The decrease of the fitting error by a factor of 3 demonstrates that, for the linoleum, the new BRDF is better suited to approximate the measured data. Figure 9 shows the measured BRDF data together with the fits obtained from the new BRDF for incidence angles from 25° to 75° every 10°.

Figure 10 shows a test scene for comparing the Ward-Dür BRDF f_{WD} to the proposed BRDF f_{new}. The scene contains an isotropic red linoleum sphere that is modeled with the particular parameters from Table 1. Because the differences between the highlights in Figures 10(a) and 10(b) are hardly visible, a close-up of the right highlight was rendered. Figure 11 shows the results obtained from using the Ward-Dür BRDF (Figure 11(a)) and the new BRDF (Figure 11(b)). The falsecolor image below (Figure 11(c)) gives the relative brightness differences between the two images with Figure 11(a) (Ward-Dür BRDF) being the reference. Here the maximal differences are located on a circular ring around the center of the highlight.

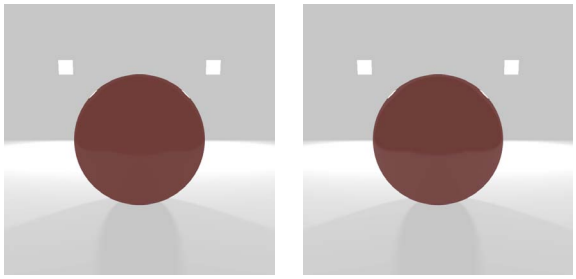

(a) (b)

Figure 10: *Test scene containing an isotropic red linoleum sphere. The specular highlights are calculated (a) by the Ward-Dür BRDF and (b) by the new BRDF.*

Compared to the Ward-Dür BRDF the new BRDF yields more expanded specular highlights and thus up to five times

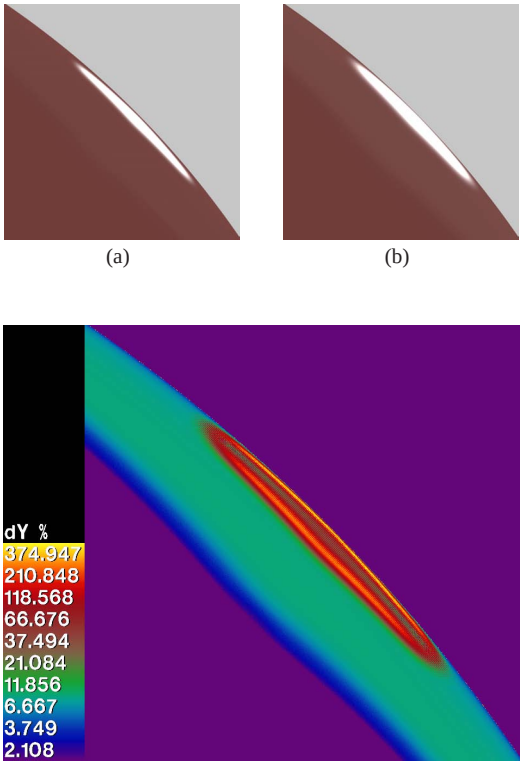

(a) (b) (c)

Figure 11: *Close-up of the right highlights in Figure 10: renderings with specular highlights calculated (a) by the Ward-Dür BRDF and (b) by the new BRDF, and (c) relative brightness differences with Ward-Dür BRDF being the reference.*

brighter reflections in off-center regions. Regarding the criticism by Ngan et al. [NDM05] that at grazing angles the Ward-Dür BRDF produces much less pronounced highlights than the measured data, the behaviour of our proposed BRDF seems to be desirable.

5. Conclusion

We presented a new BRDF model based on the Ward-Dür BRDF [Dür06]. The proposed model is physically plausible, i.e., it satisfies Helmholtz reciprocity and meets energy balance. For realistic roughness values up to 0.25 and for non-flat angles the new BRDF is very close to the Ward-Dür BRDF. Ward's sampling method gives an efficient importance sampling formula and the evaluation of both the new BRDF and the weighting factors for the Monte Carlo integration is computationally cheap. In the rendered test scenes the computation times did not observably change when using the new BRDF and weighting factors.

For a red linoleum floor from a real-world building the proposed model proved to be better suited for fitting the measured BRDF data. Using a cosine-weighted least squares approach, the fitting error decreased by a factor of 7 compared to the Ward BRDF and by a factor of 3 compared to the Ward-Dür BRDF. For the proposed model the estimated parameters yield more expanded specular highlights and up to five times brighter reflections in off-center regions.

Acknowledgments

The authors thank Christian Knoflach and Rico Thetmeyer from our cooperation partner Bartenbach LichtLabor in Aldrans, Austria, for the red linoleum measurement data. The reviewers' detailed comments that helped to improve this paper are gratefully acknowledged. Parts of this research were supported by the FIT-IT Program of the BMVIT (Bundesministerium für Verkehr, Innovation und Technologie) and the FFG with Grant No. 816009.

Appendix

In Section 3 we state that, in the plane of incidence, the maximum of the BRDF $f_{new}(\theta_l, \theta_l; \theta_v, \varphi_v)$ occurs below the mirror direction, whereas the peak of the BRDF times the cosine of the polar angle of the reflected direction $f_{new}(\theta_l, \theta_l; \theta_v, \varphi_v)\cdot\cos\theta_v$ is located in the mirror direction.

Let $\varphi_s = 1$ and $\theta_l > 0$. In the plane of incidence $\varphi_v = \varphi_l +$ and hence

$$f_{new}(\theta_l, \theta_l; \theta_v, \varphi_l +) = \frac{1}{\cdot} \cdot \frac{2(1+\cos(\theta_l + \theta_v))}{(\cos\theta_l + \cos\theta_v)^4} \cdot \exp\left(-\left(\frac{\cos^2\theta_l}{2} + \frac{\sin^2\theta_l}{2}\right)\left(\frac{\sin\theta_v - \sin\theta_l}{\cos\theta_l + \cos\theta_v}\right)^2\right). \quad (21)$$

Partial differentiation with respect to θ_v yields

$$\left.\frac{\partial f_{new}(\theta_l, \theta_l; \theta_v, \varphi_l +)}{\partial \theta_v}\right|_{\theta_v = \theta_l} = \frac{1}{4} \cdot \frac{\sin\theta_l}{\cos^3\theta_l} > 0. \quad (22)$$

Thus $f_{new}(\theta_l, \theta_l; \theta_v, \varphi_l +)$ is still increasing in the mirror direction $\theta_v = \theta_l$ and must have its maximum below. Using the product rule and applying Equation (12) we find that

$$\left.\frac{\partial (f_{new}(\theta_l, \theta_l; \theta_v, \varphi_l +)\cdot\cos\theta_v)}{\partial \theta_v}\right|_{\theta_v = \theta_l} = \frac{1}{4} \cdot \frac{\sin\theta_l}{\cos^2\theta_l} - f_{new}(\theta_l, \theta_l; \theta_l, \varphi_l +)\cdot\sin\theta_l = 0. \quad (23)$$

Thus $f_{new}(\theta_l, \theta_l; \theta_v, \varphi_v +)\cdot\cos\theta_v$ attains its maximum in the mirror direction $\theta_v = \theta_l$.

In Section 3 we state that the albedo of the new BRDF is close to 1 for small roughness values and non-flat angles, and converges to 1 for $\theta_l \to \pi/2$. Rewriting Equation (13) with respect to the sampling PDF $\mathrm{d}\omega_i$ (see Equations (14) and (15)) yields

$$a(\vec{v}) = \int_0^{2\pi}\int_0^{\pi/2} \frac{2}{1+\cos\theta_v/\cos\theta_l} \cdot \mathrm{d}\omega_i(\theta_l, \theta_l; \theta_v, \varphi_v)\cos\theta_l \sin\theta_l \,\mathrm{d}\theta_l \,\mathrm{d}\varphi_l. \quad (24)$$

Let $= \tan\Delta$ and $,\Delta$ as given by Ward's sampling method (see Equation (6)). From the spherical coordinates

$$\vec{v} = (\sin\ _v\cos\ _v, \sin\ _v\sin\ _v, \cos\ _v),$$
$$\vec{h} = (\ \cos\ ,\ \sin\ ,1)/\sqrt{1+\ ^2}, \tag{25}$$
$$\text{and}\quad \vec{l} = (\sin\ _l\cos\ _l, \sin\ _l\sin\ _l, \cos\ _l) = -\vec{v} + 2\langle\vec{h},\vec{v}\rangle\vec{h}$$

we compute

$$\frac{\cos\ _l}{\cos\ _v} = \frac{1-\ ^2+2\ \tan\ _v\cos(\ -\ _v)}{1+\ ^2}. \tag{26}$$

By the transformation law for densities and by substituting Equation (26) into Equation (24) it follows that

$$a(\vec{v}) = \iint_D \frac{2}{1+(1+\ ^2)/(1-\ ^2+2\ \tan\ _v\cos(\ -\ _v))}\mathrm{d}s\mathrm{d}t. \tag{27}$$

Here

$$D = \{(s,t)\in[0,1)^2 \,|\, 1-\ ^2+2\ \tan\ _v\cos(\ -\ _v) > 0\} \tag{28}$$

denotes the feasible domain where $_l < \ /2$ and thus a sample ray is not rejected.

In the general case, i.e. when is small and at non-flat angles where $\tan\ _v$ is not too large, the albedo is close to 1:

$$a(\vec{v}) \approx \iint_{[0,1)^2} \frac{2}{1+1}\mathrm{d}s\mathrm{d}t = 1. \tag{29}$$

For grazing angles, let $\neq 0$ and $_v \to \ /2$. Then

$$\frac{2}{1+(1+\ ^2)/(1-\ ^2+2\ \tan\ _v\cos(\ -\ _v))} \to 2 \tag{30}$$

and

$$D \to \{(s,t)\in[0,1)^2 \,|\, \cos(\ -\ _v) > 0\}. \tag{31}$$

Although in general is not uniformly distributed in $(-\ ,\ ]$, the probability that a sample ray is not rejected

$$\mathrm{P}\{\cos(\ -\ _v) > 0\} = 1/2 \tag{32}$$

because the distribution of is point symmetric about the origin. Combining Equation (27) with Equations (30) to (32) implies that $a(\vec{v}) \to 1$ if $_v \to \ /2$.

References

[AS00] ASHIKHMIN M., SHIRLEY P.: An anisotropic phong brdf model. *Journal of Graphics Tools 5* (2000), 25–32.

[Bli77] BLINN J. F.: Models of light reflection for computer synthesized pictures. *SIGGRAPH Comput. Graph. 11*, 2 (1977), 192–198.

[BS63] BECKMANN P., SPIZZICHINO A. (Eds.): *The Scattering of Electromagnetic Waves from Rough Surfaces*. Pergamon Press, NY, 1963.

[CIE04] CIE: *Colorimetry*. 3rd ed., CIE Publication 15:2004, 2004.

[CT81] COOK R. L., TORRANCE K. E.: A reflectance model for computer graphics. In *SIGGRAPH '81: Proceedings of the 8th annual conference on Computer graphics and interactive techniques* (New York, NY, USA, 1981), ACM, pp. 307–316.

[Dür04] DÜR A.: Computer Visualization. Technical Report for TICNet-Project IT-002-2003, Department of Mathematics, University of Innsbruck, 2004.

[Dür06] DÜR A.: An Improved Normalization for the Ward Reflectance Model. *Journal of Graphics Tools 11*, 1 (2006), 51–59.

[GMD10] GEISLER-MORODER D., DÜR A.: Bounding the Albedo of the Ward Reflectance Model. University of Innsbruck, Technical Report, March 2010.

[HTSG91] HE X. D., TORRANCE K. E., SILLION F. X., GREENBERG D. P.: A comprehensive physical model for light reflection. *SIGGRAPH Comput. Graph. 25*, 4 (1991), 175–186.

[KSKK10] KURT M., SZIRMAY-KALOS L., KŘIVÁNEK J.: An anisotropic brdf model for fitting and monte carlo rendering. *SIGGRAPH Comput. Graph. 44*, 1 (2010), 1–15.

[Lew94] LEWIS R. R.: Making shaders more physically plausible. *Computer Graphics Forum (Eurographics '94 Conference Issue) 13*, 3 (1994), 1–13.

[LFTG97] LAFORTUNE E. P. F., FOO S.-C., TORRANCE K. E., GREENBERG D. P.: Non-linear approximation of reflectance functions. In *SIGGRAPH '97: Proceedings of the 24th annual conference on Computer graphics and interactive techniques* (1997), pp. 117–126.

[NDM05] NGAN A., DURAND F., MATUSIK W.: Experimental Analysis of BRDF Models. In *Proc. of Eurographics Symposium on Rendering EGSR'05* (2005), pp. 117–126.

[NNSK98] NEUMANN L., NEUMANN A., SZIRMAY-KALOS L.: New Simple Reflectance Models for Metals and other Specular Materials. Vienna University of Technology, Technical Report, TR-186-2-98-17, 1998.

[NNSK99] NEUMANN L., NEUMANN A., SZIRMAY-KALOS L.: Compact metallic reflectance models. *Computer Graphics Forum 18* (1999), 161–172.

[NRH*77] NICODEMUS F. E., RICHMOND J. C., HSIA J. J., GINSBER I. W., LIMPERIS T.: *Geometrical Considerations and Nomenclature for Reflectance*. NBS Monograph 160, U. S. Dept. of Commerce, 1977.

[Pho75] PHONG B. T.: Illumination for computer generated pictures. *Commun. ACM 18*, 6 (1975), 311–317.

[Rad10] RADIANCE KNOWLEDGE DATABASE: Project web page. http://www.radiance-online.org, April 6, 2010.

[Sch94] SCHLICK C.: An Inexpensive BRDF Model for Physically-Based Rendering. *Computer Graphics Forum 13*, 3 (1994), 233–246.

[TS67] TORRANCE K. E., SPARROW E. M.: Theory for off-specular reflection from roughened surfaces. *J. Opt. Soc. Am. 57*, 9 (1967), 1105–1112.

[Wal05] WALTER B.: Notes on the Ward BRDF. Technical Report PCG-05-06, Cornell Program of Computer Graphics, available on: http://www.graphics.cornell.edu/~bjw/wardnotes.pdf, 2005.

[War92] WARD G. J.: Measuring and Modeling Anisotropic Reflection. *Computer Graphics 26*, 2 (1992), 265–272.

[War94] WARD G. J.: The RADIANCE lighting simulation and rendering system. In *SIGGRAPH '94 Proceedings* (New York, NY, USA, 1994), ACM, pp. 459–472.

[Whi80] WHITTED T.: An improved illumination model for shaded display. *Commun. ACM 23*, 6 (1980), 343–349.

[WS98] WARD G., SHAKESPEARE R.: *Rendering with Radiance*. Morgan Kaufmann Publishers, 1998.